Testing the LMA solution with solar neutrinos independently of solar models

V. Barger[1], D. Marfatia[2] and K. Whisnant[3]

[1]*Department of Physics, University of Wisconsin, Madison, WI 53706*

[2]*Department of Physics and Astronomy, University of Kansas, Lawrence, KS 66045*

[3]*Department of Physics, Iowa State University, Ames, IA 50011*

Abstract

We perform a comparative study of two methods of determining the survival probabilities of low, intermediate, and high energy solar neutrinos that emphasizes the general agreement between the Large Mixing Angle (LMA) solution and extant solar neutrino data. The first analysis is oscillation parameter-independent and the second analysis involves an approximate calculation of the survival probabilities in the three energy ranges that depends only on oscillation parameters. We show that future experiments like BOREXino, CLEAN, Heron, LENS and MOON, that measure pp and ^{7}Be neutrinos, will facilitate a stringent test of the LMA solution independently of the Standard Solar Model (SSM), without recourse to earth-matter effects. Throughout, we describe the role of SSM assumptions on our results. If the LMA solution passes the test without needing to be modified, it may be possible to establish that θ_x is nonzero at more than 2σ assuming the SSM prediction for the pp flux is correct.

1 Introduction

The LMA solution to the solar neutrino problem has emerged as the preferred explanation of solar neutrino data [1, 2]. Reactor neutrino data from the KamLAND experiment [3] have lent much confidence in this solution [4]. Nevertheless, it has long been recognized that the LMA solution is not in wholly satisfactory agreement with solar neutrino data [1]. Since the media traversed by neutrinos incident at KamLAND and at solar neutrino experiments are considerably different, it is important to confirm that the LMA solution with matter effects dictated by the MSW mechanism is consistent with solar neutrino data. Recent work emphasizing our ignorance of neutrino-matter interactions and suggestions on how solar data can help illuminate the nature of these interactions can be found in Ref. [5].

For the LMA solution, the Chlorine measurement [6], with its non-negligible component of ^{7}Be neutrinos, is too low to be consistent with the SuperKamiokande [7] (SuperK) and SNO [8] measurements of the ^{8}B neutrinos. The Small Mixing Angle solution can accommodate a low survival probability of ^{7}Be neutrinos, but at the expense of a highly non-uniform suppression of the ^{8}B neutrinos relative to the SSM [9] spectrum, which is contradicted by SuperK and SNO data. Exotic mechanisms have been proposed to account for the suppression of the ^{7}Be neutrinos, but these require that either a sterile neutrino be added [10] to the standard three-neutrino framework or that neutrino masses vary with density [11].

In this Letter we perform a model-independent analysis of the latest solar neutrino data with the flux normalizations and survival probabilities of the low, intermediate, and high energy neutrinos all treated as independent parameters; the possibility of a model-independent test of the SSM was emphasized early on in Ref. [12]. We then determine which of these parameters are calculable from current data and which require additional input from the SSM. The results of this analysis are then used to test the LMA predictions for neutrinos in each energy range. We show that with the predictions of the latest SSM and including the latest SNO salt data [13] the agreement between the LMA solution and the solar data remains relatively good, although there are minor discrepancies between the oscillation probabilities of the low- and intermediate-energy solar neutrinos which cannot be resolved by extending the analysis to include the mixing of a third neutrino. We demonstrate that future solar

neutrino experiments that would measure low and intermediate energy neutrinos and reduce the uncertainties in the survival probabilities will provide a critical test of the LMA solution.

2   Current data

2.1   Model independent analysis

2.1.1   Formalism

We use the following notation: R is the ratio of the measured rate to the SSM prediction for a given experiment, β is a flux normalization relative to the SSM, and P_L, P_I and P_H are average survival probabilities of low energy (pp), intermediate energy (^{7}Be, pep, ^{15}O, ^{13}N) and high energy (^{8}B, hep) neutrinos, respectively. For three active neutrinos and the recently updated SSM [9], the relative rates are given by

$$R_{Ga} = 0.109\beta_H P_H + 0.335\beta_I P_I + 0.556\beta_L P_L \,, \tag{1}$$

$$R_{Cl} = 0.803\beta_H P_H + 0.197\beta_I P_I \,, \tag{2}$$

$$R_{SNO}^{CC} = \beta_H P_H \,, \tag{3}$$

$$R_{SNO}^{NC} = \beta_H \,. \tag{4}$$

Here, CC and NC refer to charged-current and neutral-current measurements, respectively. See Refs. [14, 15] for a description of the method. The present measurements of these quantities are given in Table 1. The elastic scattering rates at SuperK and SNO are not included since they provide redundant information with less precision than R_{SNO}^{CC} and R_{SNO}^{NC}, although in principle these data could also be included to improve the accuracy.

2.1.2   Without SSM constraints

The quantities $\beta_L P_L$, $\beta_I P_I$ and $\beta_H P_H$ are determined from the CC measurements R_{Ga}, R_{Cl} and R_{SNO}^{CC}. R_{SNO}^{NC} determines β_H. Using the data in Table 1, we find

$$\beta_L P_L = 0.69 \pm 0.11 \,, \tag{5}$$

$$\beta_I P_I = 0.37 \pm 0.15 \,, \tag{6}$$

Table 1: Current solar neutrino measurements.

Measurement	value	source
R_{Ga}	0.54 ± 0.03	SAGE/GALLEX/GNO [16]
R_{Cl}	0.31 ± 0.03	Homestake [6]
R_{SNO}^{CC}	0.30 ± 0.01	SNO D_2O phase, SNO salt phase [8, 13]
R_{SNO}^{NC}	0.88 ± 0.06	SNO D_2O phase, SNO salt phase [8, 13]

$$\beta_H P_H = 0.30 \pm 0.01 \,, \tag{7}$$

$$\beta_H = 0.88 \pm 0.06 \,, \tag{8}$$

where the uncertainties are 1σ. Then,

$$P_H = R_{SNO}^{CC}/R_{SNO}^{NC} = 0.34 \pm 0.03 \,. \tag{9}$$

We note that P_H would not be determined by R_{SNO}^{CC} and R_{SNO}^{NC} alone if there were a fourth, sterile neutrino since the expression for R_{SNO}^{NC} would depend on the sterile content of the oscillating neutrinos [15]. At present there are no data that can determine β_L and P_L (or β_I and P_I) separately in a completely model-independent way without imposing SSM constraints.

2.1.3 With SSM constraints

The 1σ fractional uncertainties of the solar neutrino fluxes from the SSM [9] are

$$\delta(\beta_L^{SSM}) = 0.010 \,, \tag{10}$$

$$\delta(\beta_I^{SSM}) = 0.122 \,, \tag{11}$$

$$\delta(\beta_H^{SSM}) = 0.163 \,. \tag{12}$$

The values of P_L and P_I can be determined from current data only if the SSM constraints are used; from Eqs. (5, 6, 10) and (11) we deduce

$$P_L = 0.69 \pm 0.11 \quad \text{with SSM flux} \,, \tag{13}$$

$$P_I = 0.37 \pm 0.16 \quad \text{with SSM flux} \,. \tag{14}$$

4

If the SSM prediction for β_H is used as an additional constraint, then a combination of the SSM and R_{SNO}^{NC} gives

$$\beta_H = 0.89 \pm 0.06 \,, \tag{15}$$

from which we deduce

$$P_H = 0.34 \pm 0.03 \,. \tag{16}$$

2.2   LMA analysis

2.2.1   Formalism

If the ν_e disappearance of solar neutrinos occurs via the MSW mechanism [17] with adiabatic propagation [18] (which is the situation for the LMA solution), the solar neutrino oscillation probability in a three-neutrino framework is given by the approximate formula [19][1],

$$P = c_x^4 \left[\frac{1 + \cos 2\theta_s^m \cos 2\theta_s}{2} \right] + s_x^4 \,. \tag{17}$$

The above equation applies when θ_x is small, as is indicated by the CHOOZ experiment [21]; the 95% C. L. is $\sin^2 \theta_x \lesssim 0.05$ for the best-fit atmospheric mass-squared difference of 0.0021 eV^2 from the SuperK experiment [22]. For the current range of LMA parameters preferred by data, earth-matter effects [23] are very small [7, 8] and therefore we do not consider them here. The quantity in the square brackets is the two-neutrino oscillation probability and the factors involving θ_x are the corrections due to mixing with the third neutrino. The angle θ_s^m is the mixing angle in matter at the point of origin of the neutrino, and is given by

$$\tan 2\theta_s^m = \frac{\sin 2\theta_s}{\cos 2\theta_s - \hat{A}} \,, \tag{18}$$

where

$$\hat{A} \equiv \frac{2\sqrt{2} G_F N_e^0 E_\nu c_x^2}{\delta m_s^2} \simeq 1.9 \times 10^{-3} \left(\frac{E_\nu}{1 \text{ MeV}} \right) \left(\frac{8 \times 10^{-5} \text{ eV}^2}{\delta m_s^2} \right) \left(\frac{N_e^0}{N_A/\text{cm}^3} \right) c_x^2 \,. \tag{19}$$

The initial electron densities at the neutrino source are approximately $N_e^0/(N_A/\text{cm}^3) = 106$, 86 and 58 for the high, intermediate and low energy neutrinos, for which the corresponding

---

[1] In our notation, δm_s^2 is the solar mass-squared difference and θ_s and θ_x are the mixing angles conventionally denoted by θ_{12} and θ_{13}, respectively [20].

average neutrino energies are 9.06, 0.862, and 0.325 MeV, respectively. The factor c_x^2 in $\hat{A}$ is a three-neutrino correction to the effective electron number density [19]. In the LMA analysis with three neutrinos, the variables that determine the probabilities are therefore δm_s^2, θ_s and θ_x, instead of the oscillation parameter-independent probabilities P_j.

2.2.2 Without SSM constraints

As discussed in the model-independent analysis, neutrino data alone cannot presently determine P_L or P_I, so these probabilities cannot be used to constrain the LMA parameters. However, the SNO CC and NC data can be used to determine P_H, and θ_s can then be determined via Eqs. (17–19) if a range of δm_s^2 is used as input and we ignore θ_x. Taking the 1σ range, $\delta m_s^2 = (7.9 \pm 0.55) \times 10^{-5}$ eV^2, from KamLAND data [3], we find

$$\tan^2 \theta_s = 0.45 \pm 0.06, \tag{20}$$

in good agreement with recent global fits to θ_s that also include day/night spectral shapes in the analysis [24]. If θ_x is allowed to be nonzero, θ_s can be calculated as a function of θ_x; see Fig. 1. An increasing θ_s can be compensated by an increasing θ_x.

Since β_L and β_I are as yet undetermined by the data, we can use the LMA prediction for P_L and P_I in conjunction with the current best-fit values of $\beta_L P_L$ and $\beta_I P_I$ from Eqs. (5) and (6) to solve for β_L and β_I (see Fig. 2); the LMA predictions assume the 1σ ranges, $\delta m_s^2 = (7.9 \pm 0.55) \times 10^{-5}$ eV^2 from KamLAND and $\tan^2 \theta_s = 0.45 \pm 0.06$ from Eq. (20). We see that the flux normalization of the low (intermediate) energy neutrinos needs to be slightly higher (lower) in order for the LMA predictions to be completely consistent with current data, although the present uncertainties are sufficiently large that there is essentially no conflict.

2.2.3 With SSM constraints

The LMA predictions for the solar neutrino survival probability versus neutrino energy are shown in Fig. 3 for $\sin^2 \theta_x = 0$ and 0.05 with δm_s^2 and θ_s varying over their currently preferred ranges. Current data (taken from Eqs. 9, 13 and 14) are also shown, where the SSM constraints in Eqs. (10) and (11) have been used to determine P_L and P_I. The oscillation

probability of the low-energy (intermediate-energy) neutrinos is slightly higher (lower) than the LMA prediction, although the discrepancies are currently only at the 1σ level. Increasing θ_x lowers the LMA curve, which improves the fit to the intermediate energy data, but at the expense of a worse fit to the low energy data. Therefore reductions in the uncertainties from future solar neutrino experiments will provide a critical test of the LMA solution (see Sec. 3).

Using the LMA expressions for P_L, P_I and P_H, contours of constant δm_s^2 and $\tan^2 \theta_s$ are plotted in Fig. 4 in the (P_H, P_L) and (P_H, P_I) planes for $\sin^2 \theta_x = 0$ and 0.05. The data points and larger error bars are taken from Eqs. (9, 13) and (14), and the smaller error bars illustrate the expected uncertainties from future measurements of R_{pp}^{CC}, R_{pp}^{ES}, R_{Be}^{CC}, R_{Be}^{ES}, R_{SNO}^{CC} and R_{SNO}^{NC} with SSM constraints imposed (see the next section). The effect of increasing θ_x on the compatability of the LMA solution with the data is evident.

3   Future data

3.1   Model independent analysis

3.1.1   Without SSM constraints

Future experiments such as MOON [25] or LENS [26] or will be able to provide better measurements of CC scattering of the low and intermediate energy neutrinos, *i.e.*, of

$$R_{pp}^{CC} = \beta_L P_L \,, \tag{21}$$

$$R_{Be}^{CC} = \beta_I P_I \,, \tag{22}$$

perhaps at the 2.5% level [27]. However, these measurements will still not separate the flux normalization from the survival probability. In order to determine the flux normalization from data alone (*i.e.*, without imposing theoretical inputs from the SSM), a process with a NC component must be used, such as the elastic scattering (ES) measurements at BOREXino [28], CLEAN [29], HERON [30] and KamLAND [31]. They will measure

$$R_{pp}^{ES} = \beta_L P_L (1 - r_L) + \beta_L r_L \,, \tag{23}$$

$$R_{Be}^{ES} = \beta_I P_I (1 - r_I) + \beta_I r_I \,, \tag{24}$$

Table 2: Expected uncertainties from future solar neutrino measurements of CC, NC and ES processes.

	pp	^{7}Be	^{8}B
CC	2.6%	2.5%	3.5%
NC	–	–	4.8%
ES	1.1%	2.6%	–

where r_j is the ratio of the NC to ν_e cross-sections for scattering off electrons in the appropriate energy regime. CLEAN plans to measure R_{pp}^{ES} to 1.1% and R_{Be}^{ES} to 2.6%, HERON plans to measure R_{pp}^{ES} to 3.5%, and BOREXino plans to measure R_{Be}^{ES} to 5% [27]. KamLAND can measure R_{Be}^{ES} to about 11% [31]. Once R_{pp}^{ES} and R_{Be}^{ES} are measured, all six parameters (three flux normalizations and three survival probabilities) will be determined by neutrino data. Furthermore, SNO expects to reduce the uncertainties on its CC and NC measurements to about 5.5% and 6.4%, respectively, in its third phase [32]. When combined with its previous measurements, the SNO uncertainties will be about 3.5% and 4.8%, respectively. The future expectations for these uncertainties are summarized in Table 2, where we list the smallest uncertainty in each channel.

The pp measurements can be used to determine β_L and P_L via

$$\beta_L = \left[R_{pp}^{ES} - R_{pp}^{CC}(1 - r_I) \right] / r_I \,, \tag{25}$$

$$P_L = R_{pp}^{CC} r_I / \left[R_{pp}^{ES} - R_{pp}^{CC}(1 - r_I) \right] \,, \tag{26}$$

and similarly β_I and P_I can be determined from R_{Be}^{ES} and R_{Be}^{CC}. Using the six measurements R_{pp}^{CC}, R_{Be}^{CC}, R_{SNO}^{CC}, R_{SNO}^{NC}, R_{pp}^{ES} and R_{Be}^{ES} with the projected uncertainties shown in Table 2, the values of β_L, β_I and β_H can be determined independently from any solar model assumptions, with uncertainties of about 16%, 22% and 5%, respectively, assuming the central values of the $\beta_j P_j$ and β_H remain about the same (Eqs. 5–8) and that the best-fit values of β_L and β_I are close to unity. The constraints on β_L and β_I are not nearly as precise as the pp and ^{7}Be measurements themselves because the NC component, from which the value of β is inferred, is suppressed by the smaller NC cross-section for ν_μ and ν_τ, compared to the ES cross-section for ν_e. The resulting uncertainties of P_L, P_I and P_H would be about 14%, 12% and 6%,

respectively, if solar model constraints are not imposed.

3.1.2 With SSM constraints

In the future, using the CC measurements of the pp and ^{7}Be neutrinos to better determine $\beta_L P_L$ and $\beta_I P_I$, respectively, the uncertainties of P_L and P_I will be reduced to 3% and 11%, respectively, when the SSM constraints are used; the uncertainty of P_I does not improve much since the SSM intermediate energy flux is known to only 12%. The large SSM uncertainty of β_H in Eq. (12) does not provide any appreciable reduction in the overall uncertainty of β_H when combined with SNO NC data.

3.2 LMA analysis

3.2.1 Without SSM constraints

Once the six measurements in Table 2 are made, the six parameters β_L, β_I, β_H, δm_s^2, θ_s and θ_x will in principle be determined from R_{SNO}^{CC}, R_{SNO}^{NC}, R_{Be}^{CC}, R_{Be}^{ES}, R_{pp}^{CC} and R_{pp}^{ES}, without needing any other inputs such as SSM fluxes or KamLAND data.

Figure 5 shows contours of constant θ_s and θ_x in two-dimensional subspaces of probability space for $\delta m_s^2 = 8 \times 10^{-5}$ eV^2. The current best fit values for these parameters are also shown in the figure. The central value of P_L is accommodated only for $\sin^2 \theta_x < 0$, which is unphysical, while the central value of P_I is accommodated for values of $\sin^2 \theta_x$ that violate the CHOOZ bound. However, there is adequate consistency within error bars. As noted earlier, if the flux normalizations β_L and β_I of the SSM are correct, then the current central values of P_L and P_I are slightly high and low, respectively. Future solar neutrino measurements will be able to provide a more definitive statement about this minor discrepancy, even without making any SSM assumptions. It is also clear from Fig. 5 that a more precise *experimental* determination of β_I and especially β_L would be needed to provide significant improvements in the determination of oscillation parameters if the predictions of the SSM are not used.

3.2.2 With SSM constraints

In the future, after R_{pp}^{CC} is measured and the SSM constraint (Eq. 10) is imposed, P_L would be determined to about 3%. These projected uncertainties are shown as the smaller error bars in Figs. 4 and 5.

With the SSM constraints imposed, measurements of $\tan^2\theta_s$ and $\sin^2\theta_x$ can be made with 1σ uncertainties of order 0.03 and 0.015, respectively, by future solar neutrino experiments. As is evident from Figs. 4 and 5, to be consistent with the LMA solution, the current central values of P_L and P_I should shift when the new measurements are made.

We note that if R_{Cl} were about 1σ higher, then both $\beta_L P_L$ and $\beta_I P_I$ would be about at the values predicted by the best-fit LMA parameters and the SSM; they are coupled together since $\beta_L P_L$ cannot be determined from R_{Ga} without knowing $\beta_I P_I$, which is determined from R_{Cl} and $\beta_H P_H = R_{SNO}^{CC}$. Since the primary constraint on $\beta_I P_I$ comes from R_{Cl}, to which $\beta_I P_I$ only makes a 20% contribution, the current determination of $\beta_I P_I$ has a large uncertainty. Future measurements of $\beta_I P_I$ in R_{Be}^{CC} will not only significantly reduce the uncertainty on $\beta_I P_I$, but also will test the Chlorine measurement.

4 Summary

We have shown that current neutrino data can determine the survival probability of only the high-energy neutrinos if SSM flux normalizations are not used, and that if the SSM flux constraints are imposed, the LMA solution provides a consistent explanation of all solar neutrino data, although minor discrepancies remain at the 1σ level. In particular, the implied flux of low (intermediate) energy neutrinos appears to be slightly high (low), if the LMA solution is correct. Including the small mixing effects of the third neutrino cannot compensate for both inconsistencies simultaneously.

Future measurements of low and intermediate energy neutrinos will provide a much stricter test of the viability of the LMA solution independently of SSM predictions for the fluxes. See Table 3 for a summary of our results. If reliance is placed in the SSM pp flux normalization, the test becomes conclusive. If the LMA solution survives without modification, it may be possible to demonstrate that θ_x is nonzero at more than 2σ.

Data	SSM imposed?	$\delta(\beta_L)$	$\delta(\beta_I)$	$\delta(\beta_H)$	$\delta(P_L)$	$\delta(P_I)$	$\delta(P_H)$
Current	No	−	−	6	−	−	8
Current	Yes	1	12	6	15	43	8
Future	No	16	22	5	14	12	6
Future	Yes	1	11	5	3	11	6

Table 3: Percentage uncertainties in the flux normalizations and survival probabilities from current and future solar neutrino measurements. From the current data, β_L and β_I (and hence P_L and P_I) cannot be determined without SSM input. For the future data we have assumed that the central values of $\beta_j P_j$ and β_H coincide with those of the current measurements (see Eqs. 5–8) and that the best-fit values of β_L and β_I are close to unity.

5   Acknowledgments

References

[1] V. Barger, D. Marfatia, K. Whisnant and B. P. Wood, Phys. Lett. B **537**, 179 (2002) [arXiv:hep-ph/0204253]; A. Strumia, C. Cattadori, N. Ferrari and F. Vissani, Phys. Lett. B **541**, 327 (2002) [arXiv:hep-ph/0205261].

[2] A. Bandyopadhyay, S. Choubey, S. Goswami and D. P. Roy, Phys. Lett. B **540**, 14 (2002) [arXiv:hep-ph/0204286]; J. N. Bahcall, M. C. Gonzalez-Garcia and C. Pena-Garay, JHEP **0207**, 054 (2002) [arXiv:hep-ph/0204314]; P. Aliani, V. Antonelli, R. Ferrari, M. Picariello and E. Torrente-Lujan, Phys. Rev. D **67**, 013006 (2003) [arXiv:hep-ph/0205053]; P. C. de Holanda and A. Y. Smirnov, Phys. Rev. D **66**, 113005 (2002) [arXiv:hep-ph/0205241]; G. L. Fogli, E. Lisi, A. Marrone, D. Montanino and A. Palazzo, Phys. Rev. D **66**, 053010 (2002) [arXiv:hep-ph/0206162].

[3] K. Eguchi *et al.* [KamLAND Collaboration], Phys. Rev. Lett. **90**, 021802 (2003) [arXiv:hep-ex/0212021]; T. Araki *et al.*, arXiv:hep-ex/0406035.

[4] See *e.g.* V. Barger and D. Marfatia, Phys. Lett. B **555**, 144 (2003) [arXiv:hep-ph/0212126].

[5] R. Fardon, A. E. Nelson and N. Weiner, arXiv:astro-ph/0309800. D. B. Kaplan, A. E. Nelson and N. Weiner, Phys. Rev. Lett. **93**, 091801 (2004) [arXiv:hep-ph/0401099]; K. M. Zurek, arXiv:hep-ph/0405141; A. Friedland, C. Lunardini and C. Pena-Garay, Phys. Lett. B **594**, 347 (2004) [arXiv:hep-ph/0402266]; M. M. Guzzo, P. C. de Holanda and O. L. G. Peres, Phys. Lett. B **591**, 1 (2004) [arXiv:hep-ph/0403134]; O. G. Miranda, M. A. Tortola and J. W. F. Valle, arXiv:hep-ph/0406280.

[6] B. T. Cleveland *et al.*, Astrophys. J. **496**, 505 (1998).

[7] S. Fukuda *et al.*, [Super-Kamiokande Collaboration] Phys. Lett. B **539**, 179 (2002) [arXiv:hep-ex/0205075]; M. B. Smy *et al.*, Phys. Rev. D **69**, 011104 (2004) [arXiv:hep-ex/0309011].

[8] Q. R. Ahmad *et al.* [SNO Collaboration], Phys. Rev. Lett. **89**, 011301 (2002) [arXiv:nucl-ex/0204008]; Phys. Rev. Lett. **89**, 011302 (2002) [arXiv:nucl-ex/0204009];

S. N. Ahmed *et al.*, Phys. Rev. Lett. **92**, 181301 (2004) [arXiv:nucl-ex/0309004]; B. Aharmim *et al.* [SNO Collaboration], arXiv:nucl-ex/0502021.

[9] J. N. Bahcall, A. M. Serenelli and S. Basu, arXiv:astro-ph/0412440; J. N. Bahcall and A. M. Serenelli, arXiv:astro-ph/0412096.

[10] P. C. de Holanda and A. Y. Smirnov, Phys. Rev. D **69**, 113002 (2004) [arXiv:hep-ph/0307266].

[11] V. Barger, P. Huber and D. Marfatia, arXiv:hep-ph/0502196.

[12] N. Hata and P. Langacker, Phys. Rev. D **52**, 420 (1995) [arXiv:hep-ph/9409372].

[13] B. Aharmim *et al.* [SNO Collaboration], arXiv:nucl-ex/0502021.

[14] V. D. Barger, R. J. N. Phillips and K. Whisnant, Phys. Rev. D **43**, 1110 (1991).

[15] V. D. Barger, D. Marfatia and K. Whisnant, Phys. Lett. B **509**, 19 (2001) [arXiv:hep-ph/0104166]; Phys. Rev. Lett. **88**, 011302 (2002) [arXiv:hep-ph/0106207].

[16] W. Hampel *et al.* [GALLEX Collaboration], Phys. Lett. B **447**, 127 (1999); M. Altmann *et al.* [GNO Collaboration], Phys. Lett. B **490**, 16 (2000) [arXiv:hep-ex/0006034]; J. N. Abdurashitov *et al.* [SAGE Collaboration], J. Exp. Theor. Phys. **95**, 181 (2002) [Zh. Eksp. Teor. Fiz. **122**, 211 (2002)] [arXiv:astro-ph/0204245].

[17] L. Wolfenstein, Phys. Rev. D **17**, 2369 (1978); V. D. Barger, K. Whisnant, S. Pakvasa and R. J. N. Phillips, Phys. Rev. D **22**, 2718 (1980); S. P. Mikheev and A. Y. Smirnov, Sov. J. Nucl. Phys. **42**, 913 (1985) [Yad. Fiz. **42**, 1441 (1985)].

[18] H. A. Bethe, Phys. Rev. Lett. **56**, 1305 (1986); W. C. Haxton, Phys. Rev. Lett. **57**, 1271 (1986); V. D. Barger, R. J. N. Phillips and K. Whisnant, Phys. Rev. D **34**, 980 (1986).

[19] T. K. Kuo and J. Pantaleone, Rev. Mod. Phys. **61**, 937 (1989); G. L. Fogli, E. Lisi, D. Montanino and A. Palazzo, xPhys. Rev. D **62**, 113004 (2000) [arXiv:hep-ph/0005261].

[20] V. Barger, D. Marfatia and K. Whisnant, Int. J. Mod. Phys. E **12**, 569 (2003) [arXiv:hep-ph/0308123].

[21] M. Apollonio *et al.* [CHOOZ Collaboration], Eur. Phys. J. C **27**, 331 (2003) [arXiv:hep-ex/0301017].

[22] Y. Ashie *et al.* [Super-Kamiokande Collaboration], arXiv:hep-ex/0501064.

[23] A. J. Baltz and J. Weneser, Phys. Rev. D **35**, 528 (1987); Phys. Rev. D **37**, 3364 (1988).

[24] A. B. Balantekin, V. Barger, D. Marfatia, S. Pakvasa and H. Yuksel, Phys. Lett. B **613**, 61 (2005) [arXiv:hep-ph/0405019]; A. Strumia and F. Vissani, arXiv:hep-ph/0503246.

[25] P. Doe *et al.*, Nucl. Phys. A **721**, 517 (2003).

[26] T. Lasserre [LENS Collaboration], Prog. Part. Nucl. Phys. **48**, 231 (2002).

[27] H. Back *et al.*, arXiv:hep-ex/0412016.

[28] G. Alimonti *et al.* [Borexino Collaboration], Astropart. Phys. **16**, 205 (2002) [arXiv:hep-ex/0012030].

[29] D. N. McKinsey and K. J. Coakley, arXiv:astro-ph/0402007.

[30] J. S. Adams, A. Fleischmann, Y. H. Huang, Y. H. Kim, R. E. Lanou, H. J. Maris and G. M. Seidel, *Prepared for International Workshop on Next Generation Nucleon Decay and Neutrino Detector (NNN 99), Stony Brook, New York, 23-25 Sep 1999.*

[31] P. Alivisatos *et al.* [KamLAND Collaboration], STANFORD-HEP-98-03.
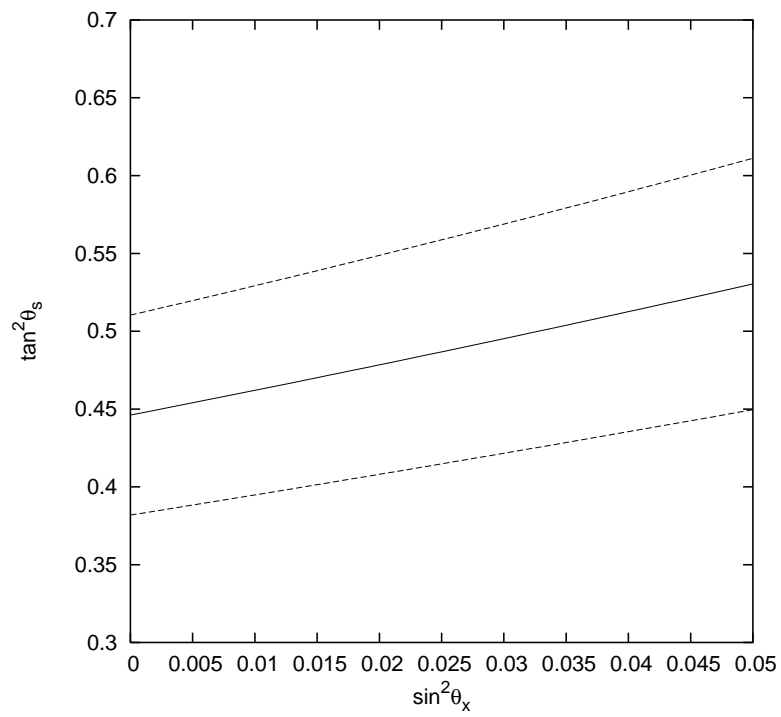
[32] A. McDonald, private communication.

Figure 1: Inferred values of $\tan^2 \theta_s$ versus $\sin^2 \theta_x$ using the current SNO data and the 1σ range, $\delta m_s^2 = (7.9 \pm 0.55) \times 10^{-5}$ eV^2, from KamLAND data alone.
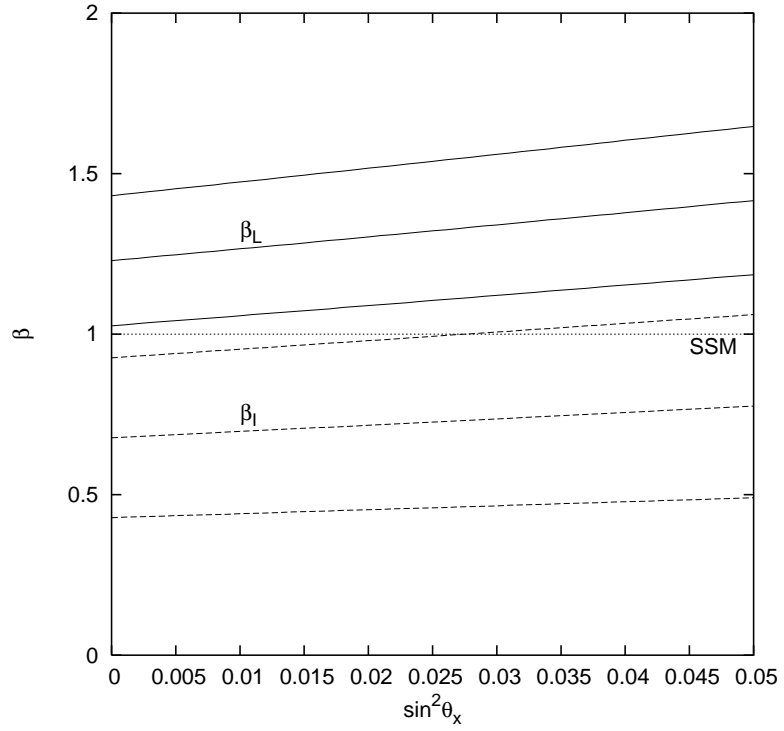
Figure 2: Inferred values of β_L (solid) and β_I (dashed) for $\delta m_s^2 = (7.9 \pm 0.55) \times 10^{-5}$ eV^2, using the LMA predictions for P_L and P_I and Eqs. (5,6). In each case the central values and 1σ error band is shown. The dotted line is the SSM prediction.
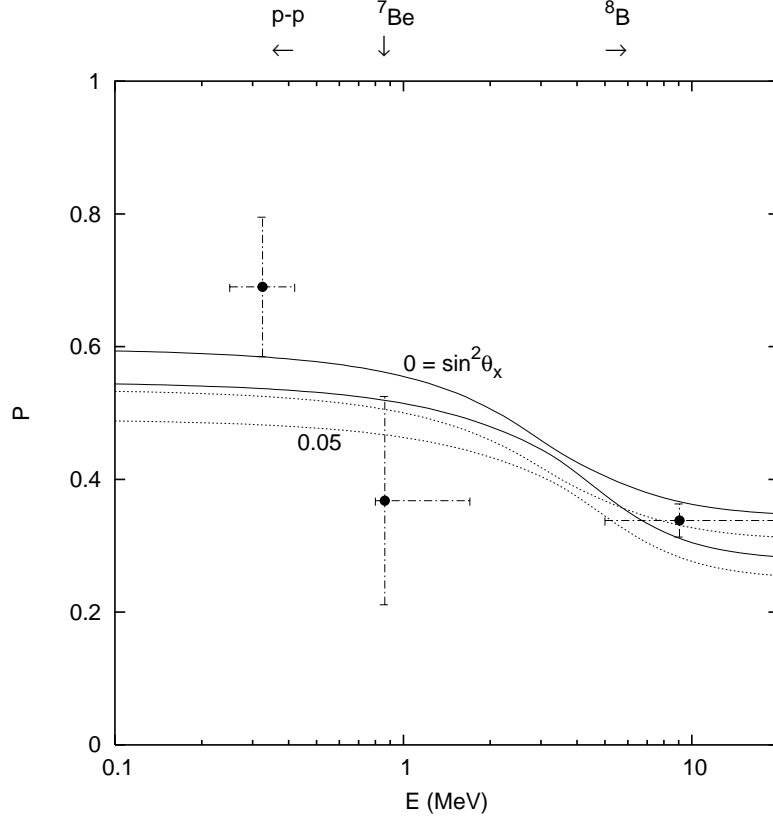
Figure 3: LMA predictions for solar neutrino survival probability versus neutrino energy for $\sin^2 \theta_x = 0$ (solid), 0.05 (dashed). The bands shows the range of predictions for $\delta m_s^2 = (7.9 \pm 0.55) \times 10^{-5}$ eV^2 and $\tan^2 \theta_s = 0.45 \pm 0.06$. The data points are taken from Eqs. (9, 13) and (14), the latter two of which were obtained using the SSM predictions for β_L and β_I.
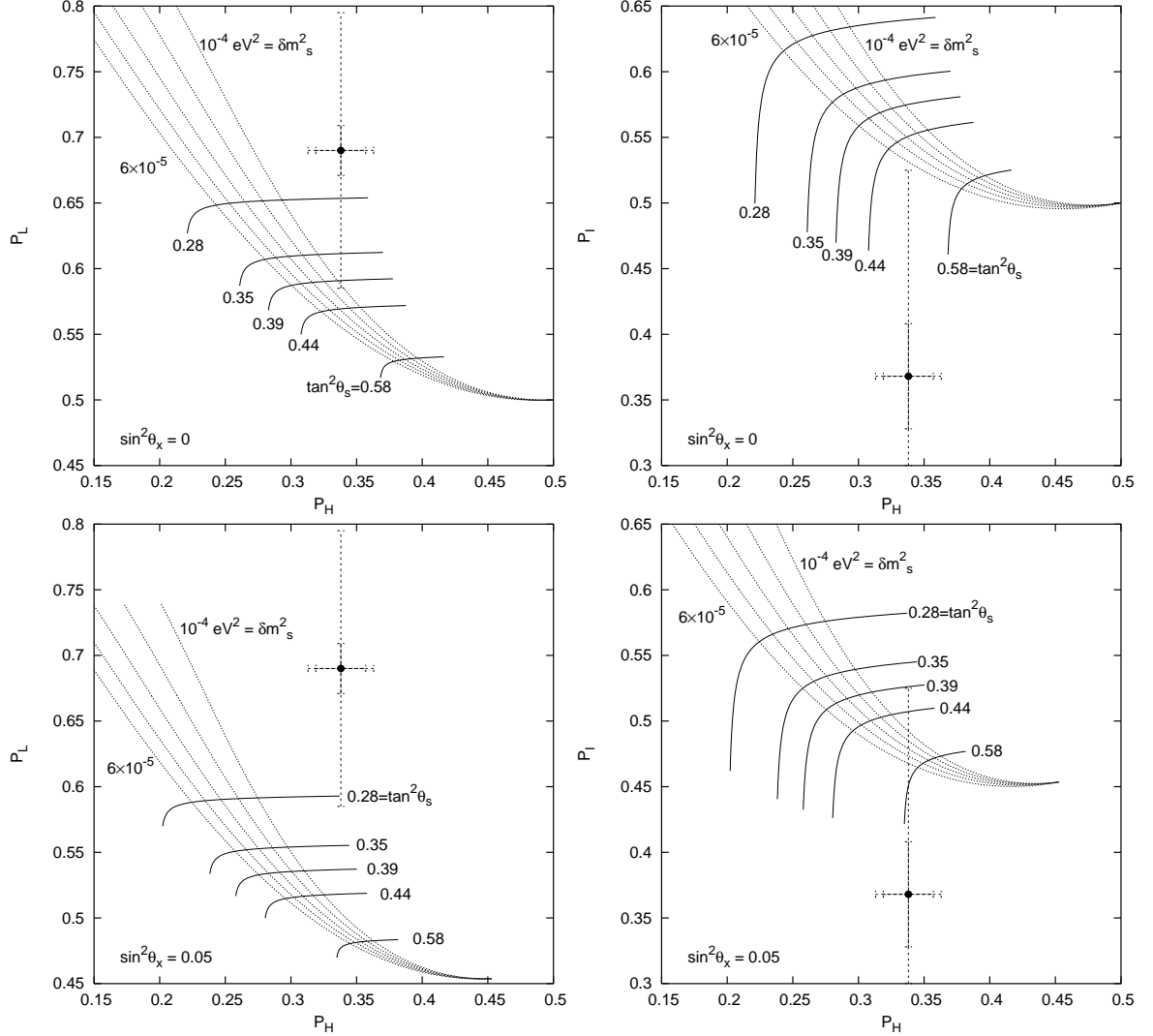
Figure 4: Contours of θ_s and δm_s^2 in the (P_H, P_L) and (P_H, P_I) planes for $\sin^2 \theta_x = 0$ and 0.05. The bold data point and larger error bars are taken from Eqs. (9, 13) and (14), the latter two of which were obtained using SSM constraints. The smaller error bars are projected improvements in the uncertainties from future measurements of R_{pp}^{CC}, R_{pp}^{ES}, R_{Be}^{CC}, R_{Be}^{ES}, R_{SNO}^{CC} and R_{SNO}^{NC} with SSM constraints imposed.
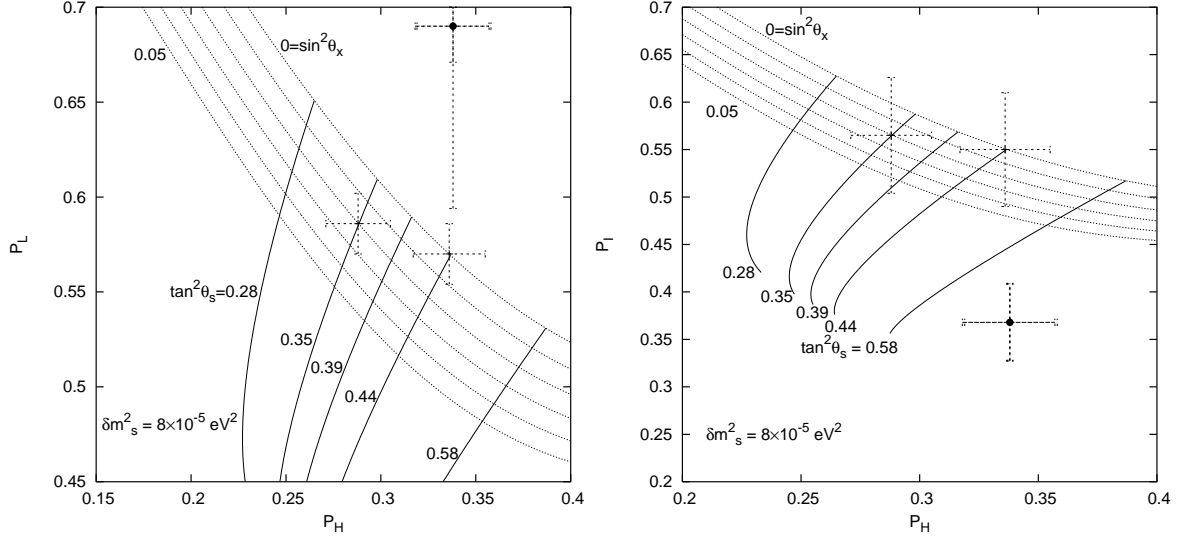
Figure 5: Contours of θ_s and θ_x in the (P_H, P_L) and (P_H, P_I) planes, for $\delta m_s^2 = 8 \times 10^{-5}$ eV^2. The bold data points are the current central values from Eqs. (9, 13) and (14). The larger (smaller) error bars are the projected uncertainties from the future measurements listed in Table 2 without (with) SSM constraints imposed. While adding SSM constraints to future data reduces the uncertainty in P_L significantly, P_I and P_H are essentially unimproved. Two representative future measurements (with SSM flux constraints) are indicated at $(\tan^2 \theta_s, \sin^2 \theta_x) = (0.35, 0.03)$ and $(0.44, 0)$.